18th International Conference
ENGINEERING MECHANICS 2012
Svratka, Czech Republic, May 14 – 17, 2012

pp. 933–944
Paper #261

MICROMECHANICS-BASED MODELS OF COCCIOPESTO MORTARS

V. Nežerka*, M. Somr, J. Zeman*****

Abstract: *The paper deals with homogenization and strength estimation of mortars containing crushed bricks or other clay products. These mortars, known as cocciopesto, were used mainly during the Byzantine period and by Romans. Cocciopesto exhibit quite extraordinary mechanical properties due to formation of C-S-H gel coating on the interface between lime matrix and crushed clay products. Based on literature study, it seems that no one has ever tried to estimate the properties of cocciopesto mortars using micromechanical modeling. The micromechanical approach and Mori-Tanaka homogenization technique provided an explanation for the characteristic behavior of these mortars, but they had to be modified for homogenization of coated particles. Mortar strength was estimated from magnitudes of the quadratic average of deviatoric strain in individual phases. The calculations confirmed the important role of the C-S-H gel coating on the mortar strength and stiffness. Despite the above mentioned simplifications and a few uncertainties, the model seems to be able to correctly predict the trends and serve for an optimization of the mortar composition towards desired properties.*

Keywords: ***cocciopesto, micromechanics, Mori-Tanaka method, C-S-H gel coating, strength estimation***

1. Introduction

The present conservation practice uses air lime or hydraulic lime mortars, because these are compatible with the original materials. The use of air lime presents problems with slow setting, inability to harden under water, lack of durability and poor mechanical strength. Therefore, the hydraulic lime-pozzolan mortars were widely used in the past and are still used nowadays for repairs. These mortars are of a higher porosity and lower strength than cement-based mortars, but they exhibit better durability.

Phoenicians were probably the first ones who added crushed clay products, such as burnt bricks, tiles or pieces of pottery, to the lime mortar in order to increase its durability and strength. Romans used this type of mortar in areas where other natural pozzolans were not available and called such material *cocciopesto*. The structures, mainly from the Byzantine period, have also very thick joints, often comparable to the size of bricks. Together with the enhanced mechanical properties of the cocciopesto mortar, the use of the thick joints probably results in the increased resistance to earthquake loading, since the non-linear behavior of the mortar allows for a better energy dissipation (Baronio et al., 1997).

By a closer investigation, it was found that the mortars containing crushed bricks exhibit a hydraulic character due to formation of C-S-H gel on the lime-brick interface. It was reported in many papers, dealing with the cocciopesto mortars, that a thin layer of the gel forms at the interface if the bricks are made of clay and burnt at the appropriate firing temperature (which is about 600-900°C (Maropoulou et al., 1995)). Since this component is responsible for some extraordinary properties of Portland cement concrete, it is conjectured that also the enhanced mechanical properties of the lime-crushed brick mortars can be attributed to the relatively high strength and stiffness of the C-S-H gel coating. The addition of crushed bricks should ensure the mortar hydraulicity, and therefore improve mechanical properties of the mortar, without the need for modern artificial substances or industrial by-products such as metakaolin or fly ash.

*Ing. Václav Nežerka: Faculty of Civil Engineering, Czech Technical University in Prague, Thákurova 7, 166 29 Praha 6, Czech Republic; e-mail: vaclav.nezerka@fsv.cvut.cz
**Ing. Michael Somr: Faculty of Civil Engineering, Czech Technical University in Prague, Thákurova 7, 166 29 Praha 6, Czech Republic; e-mail: michael.somr@fsv.cvut.cz
***Doc. Ing. Jan Zeman, Ph.D.: Faculty of Civil Engineering, Czech Technical University in Prague, Thákurova 7, 166 29 Praha 6, Czech Republic; e-mail: zemanj@cml.fsv.cvut.cz

The goal of this work is to investigate the influence of the C-S-H gel coating on the mortar behavior from the micromechanical point of view and provide a tool for the estimation mechanical properties based on mortar composition. Two works, (Pichler and Hellmich, 2011) and (Šmilauer et al., 2011), provided an inspiration for the development of micromechanical models. These works deal with composite materials, composed of a matrix, voids and aggregates and exploit the Mori-Tanaka method (Benveniste, 1987; Mori and K., 1973) to estimate the effective stiffness and strength of the composite. It is assumed that only the deviatoric stress is responsible for a failure of the material, therefore the quadratic average of the deviatoric stress in the lime matrix was chosen as an adequate indicator for the determination of mortar strength. Even though there are a few simplifications in these models, the results in Pichler and Hellmich (2011) and Šmilauer et al. (2011) quite well correspond to the available experimental data and therefore they should be applicable to the mortars with crushed bricks as well.

2. Stiffness Homogenization

The term inhomogeneity is understood as an inclusion of a material embedded in a matrix, having different material properties from those of the matrix. If a sample of an inhomogeneous material is subjected to the external load $\mathbf{E}$, then the average strain in individual phases can be calculated as $\mathbf{E}^{(r)} = \mathbf{A}^{(r)} : \mathbf{E}$, where $\mathbf{A}^{(r)}$ represents a strain concentration factor for a phase r. The superscript r attains the values from 1 (possibly even 0 if the matrix is included) to the number of phases n. The strain concentration factor can be calculated as follows:

$$\mathbf{A}_{\text{dil}}^{(r)} = [\mathbf{I} + \mathbf{S} : \mathbf{M}^{(0)} : (\mathbf{L}^{(r)} - \mathbf{L}^{(0)})]^{-1} \qquad \text{where} \qquad r = 1, ..., n \tag{1}$$

where $\mathbf{I}$ represents the fourth order unity tensor with components $I_{ijkl} = 1/2(\delta_{ik}\delta_{jl} + \delta_{il}\delta_{jk})$, where δ_{ij} is a Kronecker delta defined as $\delta_{ij} = 1$ for $i = j$, and $\delta_{ij} = 0$ otherwise; $\mathbf{S}$ is so called Eshelby tensor and its components for various inclusion shapes can be found, e.g., in Mura (1987), $\mathbf{M}^{(0)}$ is a compliance tensor representing the matrix, the $\mathbf{L}^{(r)}$ and $\mathbf{L}^{(0)}$ are stiffness tensors, representing the individual phases and the matrix, respectively.

The subscript dil in Eq. (1) stands for a "dilute distribution", because Eq. (1) is valid under the assumption that the inhomogeneity is embedded in an infinite matrix. The assumption of dilutely distributed non-interacting inhomogeneities is a starting point for a refinement of the model accounting for a mutual interaction of inhomogeneities, such as the Mori-Tanaka scheme introduced next.

2.1. Mori-Tanaka Scheme

The Mori-Tanaka model, (Benveniste, 1987; Mori and K., 1973), formally equals to that of a dilute distribution. However, the strain in individual inhomogeneities is not directly dependent on the externally applied load (macroscopic strain), but rather on a strain in the matrix, which is approximated by a constant field $\mathbf{E}^{(0)}$:

$$\mathbf{E}^{(r)} = \mathbf{A}_{\text{dil}}^{(r)} : \mathbf{E}^{(0)} \tag{2}$$

The relationship between the macroscopic strain and strain in the matrix can be found using a simple reasoning:

$$\begin{aligned} \mathbf{E} &= c^{(0)}\mathbf{E}^{(0)} + \sum_{r=1}^{n} c^{(r)}\mathbf{E}^{(r)} = c^{(0)}\mathbf{E}^{(0)} + \sum_{r=1}^{n} c^{(r)}\mathbf{A}_{\text{dil}}^{(r)} : \mathbf{E}^{(0)} = \\ &= \left(c^{(0)}\mathbf{I} + \sum_{r=1}^{n} c^{(r)}\mathbf{A}_{\text{dil}}^{(r)} \right) : \mathbf{E}^{(0)} \end{aligned} \tag{3}$$

where c, having a superscript (0) and (r), stands for a volume fraction of the matrix and inhomogeneities, respectively. The relationship between the average matrix strain and the macroscopic strain can be described simply as $\mathbf{E}^{(0)} = \mathbf{A}_{\text{MT}}^{(0)} : \mathbf{E}$, where

$$\mathbf{A}_{\text{MT}}^{(0)} = \left(c^{(0)}\mathbf{I} + \sum_{r=1}^{n} c^{(r)}\mathbf{A}_{\text{dil}}^{(r)} \right)^{-1} \tag{4}$$

is the Mori-Tanaka strain concentration factor. The strain in the individual inhomogeneities is then provided by

$$\mathbf{E}^{(r)} = \mathbf{A}_{\mathrm{dil}}^{(r)} : \mathbf{E}^{(0)} = \mathbf{A}_{\mathrm{dil}}^{(r)} : \mathbf{A}_{\mathrm{MT}}^{(0)} : \mathbf{E} \tag{5}$$

2.2. Effective Stiffness according to M-T Scheme

The relationship between the macroscopic stress $\mathbf{\Sigma}$ and strain $\mathbf{E}$ can be obtained as follows:

$$\mathbf{\Sigma} = \sum_{r=0}^{n} c^{(r)} \mathbf{\Sigma}^{(r)} = \sum_{r=0}^{n} c^{(r)} \mathbf{L}^{(r)} : \mathbf{E}^{(r)} = \sum_{r=0}^{n} c^{(r)} \mathbf{L}^{(r)} : \mathbf{A}^{(r)} : \mathbf{E} = \mathbf{L}^{\mathrm{eff}} : \mathbf{E} \tag{6}$$

where $\mathbf{L}^{\mathrm{eff}}$ is the effective stiffness tensor, and in case of the Mori-Tanaka scheme it can be obtained as

$$\mathbf{L}^{\mathrm{eff}} = \left(c^{(0)} \mathbf{L}^{(0)} + \sum_{r=1}^{n} c^{(r)} \mathbf{L}^{(r)} : \mathbf{A}_{\mathrm{dil}}^{(r)} \right) : \mathbf{A}_{\mathrm{MT}}^{(0)} \tag{7}$$

In the special case of an isotropic matrix containing isotropic spherical inhomogeneities, the Mori-Tanaka model yields an isotropic overall behavior, irrespective of the spatial arrangement of the phases. The effective stiffness of such composite can be then described by scalar constants, since the Eshelby tensor can be also decomposed into its volumetric and deviatoric part:

$$\mathbf{S} = \alpha^{(0)} \frac{1}{3} \delta_{ij} \delta_{kl} + \alpha^{(0)} \left(\mathbf{I} - \frac{1}{3} \delta_{ij} \delta_{kl} \right) = \alpha^{(0)} \mathbf{I}_{\mathrm{V}} + \beta^{(0)} \mathbf{I}_{\mathrm{D}} \tag{8}$$

where $\mathbf{I}_{\mathrm{V}}$ and $\mathbf{I}_{\mathrm{D}}$ are volumetric and deviatoric projection tensors, respectively. These tensors serve for a decomposition of any stress or strain tensor into its volumetric and deviatoric components. The scalar parameters $\alpha^{(0)}$ and $\beta^{(0)}$ depend, in case of spherical isotropic particles, only on the matrix Poisson's ratio:

$$\alpha^{(0)} = \frac{1 + \nu^{(0)}}{3\left(1 - \nu^{(0)}\right)} \qquad \text{and} \qquad \beta^{(0)} = \frac{2\left(4 - 5\nu^{(0)}\right)}{15\left(1 - \nu^{(0)}\right)} \tag{9}$$

These parameters are also called constraint constants and because of the entire isotropy (i.e., elastic and geometric) they can be expressed by scalar values. They relate the eigenstrains ε^t in individual phases to the total strain, and the decomposition into volumetric and deviatoric strain highlights their meaning:

$$\varepsilon_{kk} = \alpha \varepsilon_{kk}^t \qquad \text{and} \qquad \varepsilon_{ij} = \beta \varepsilon_{ij}^t \tag{10}$$

Using the equations (5), (8) and knowing that the elastic stiffness tensor can be decomposed into volumetric and deviatoric parts, $\mathbf{L} = 3K\mathbf{I}_{\mathrm{V}} + 2G\mathbf{I}_{\mathrm{D}}$, all the terms in Eq. (7) can be decompossed into their volumetric and deviatoric parts. Since the volumetric and deviatoric components are independent of each other, the effective bulk modulus can be, after a simple manipulation, expressed as

$$K^{\mathrm{eff}} = \frac{c^{(0)} K^{(0)} + \sum_{r=1}^{n} c^{(r)} K^{(r)} \left[1 + \alpha^{(0)} \left(\frac{K^{(r)}}{K^{(0)}} - 1 \right) \right]^{-1}}{c^{(0)} + \sum_{r=1}^{n} c^{(r)} \left[1 + \alpha^{(0)} \left(\frac{K^{(r)}}{K^{(0)}} - 1 \right) \right]^{-1}} \tag{11}$$

and the effective shear modulus as

$$G^{\mathrm{eff}} = \frac{c^{(0)} G^{(0)} + \sum_{r=1}^{n} c^{(r)} G^{(r)} \left[1 + \beta^{(0)} \left(\frac{G^{(r)}}{G^{(0)}} - 1 \right) \right]^{-1}}{c^{(0)} + \sum_{r=1}^{n} c^{(r)} \left[1 + \beta^{(0)} \left(\frac{G^{(r)}}{G^{(0)}} - 1 \right) \right]^{-1}} \tag{12}$$

2.3. Homogenization with Coated Particles

This section is devoted to the evaluation of the constraint constants for coated particles, relating the induced strain to the eigenstrain in individual phases, $\alpha^{(r)}$ and $\beta^{(r)}$, and obtaining the effective elastic properties. The spherical inclusion with a thin interlayer and embedded in a matrix is considered for the evaluation. This is an enormous simplification and it is also a good model for randomly oriented inhomogeneities, such as particles embedded in the mortar paste.

The whole procedure for a determination of the constraint constants, $\alpha^{(r)}$ and $\beta^{(r)}$ was taken from Luo and Weng (1987), where the theoretical background can be found. Motivated by Eshelby's observations, Luo and Weng (1987) undertook a similar study to find the elastic field in the inclusion (grain) and its coating, which is embedded in an infinitely extended matrix. They restricted their consideration to the case of a three-phase, spherically concentric solid. The solution of Luo and Weng is based on the equations for a general displacement field in spherical coordinates. The integration constants were found using the continuity conditions and equilibrium of stresses on the interface of individual phases.

The superscript (g) stands for the grain (or the inner inclusion), (c) stands for the coating and the superscript (m) is used in the quantities describing the surrounding matrix. The parameter c is defined as $c = (a/b)^3$ (see Fig. 1) and it has a physical meaning of the volume fraction of phases in a two-phase composite. The hydrostatic and deviatoric transformation problems are treated separately. Each phase, a grain, its coating and a surrounding matrix, is represented by its bulk modulus $K^{(r)}$ and shear modulus $G^{(r)}$. The geometry is described by the radius of a grain a and radius of its coating b, as depicted in the following figure:

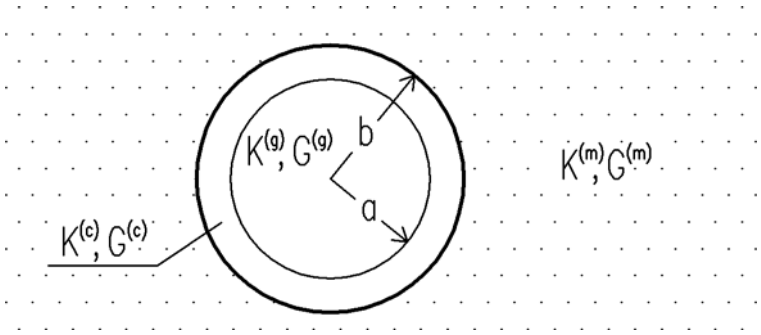

Fig. 1: A three-phase composite spherically concentric solid

Volumetric Part

The constraint constant for grain $\alpha^{(g)}$ is calculated as

$$\alpha^{(g)} = 3K^{(g)}\left[\left(3K^{(c)} + 4G^{(m)}\right) - 4c\left(G^{(m)} - G^{(c)}\right)\right]/p \tag{13}$$

where $c = (a/b)^3$ and p is

$$p = \left(3K^{(g)} + 4G^{(c)}\right)\left(3K^{(c)} + 4G^{(m)}\right) - 12c\left(K^{(g)} - K^{(c)}\right)\left(G^{(m)} - G^{(c)}\right) \tag{14}$$

The constraint constant for the coating of the grain, $\alpha^{(c)}$, is obtained as

$$\alpha^{(c)} = -4cK^{(g)}\left(G^{(m)} - G^{(c)}\right)/p \tag{15}$$

Deviatoric Part

The deviatoric constraint constant for the grain can be found in the form

$$\beta^{(g)} = a_1 - \frac{21}{5\left(1 - \nu^{(g)}\right)}\, a_2 \tag{16}$$

and for the coating as

$$\beta^{(c)} = b_1 - \frac{21}{5\left(1 - 2\nu^{(c)}\right)}\frac{1 - c^{\,5/3}}{1 - c}\, b_2 \tag{17}$$

where the constants a_1 and a_2 can be calculated as

$$\begin{pmatrix} a_1 \\ a_2 \end{pmatrix} = \mathbf{R}^{-1} \tag{18}$$

and the terms b_1 and b_2, needed for the calculation of the deviatoric constraint constants for the coating, can be found as

$$\begin{pmatrix} b_1 \\ b_2 \\ b_3 \\ b_4 \end{pmatrix} = \mathbf{E}^{-1}\mathbf{F}\mathbf{K}^{-1}\mathbf{H}\mathbf{R}^{-1} \tag{19}$$

The individual matrices, needed for the calculation of coefficients a_1, a_2 and b_1, b_2, can be found in the Appendix.

Modification of Stiffness Homogenization

For the calculation of the effective moduli, the formulas (11) and (12) can be used in a slightly modified form. Namely, the constraint constants $\alpha^{(0)}$ and $\beta^{(0)}$ are substituted by the corresponding constants $\alpha^{(r)}$ and $\beta^{(r)}$, which remain $\alpha^{(0)}$ and $\beta^{(0)}$ in case of uncoated particles. However, coated grains are represented by $\alpha^{(g)}$ and $\beta^{(g)}$ and their coating by $\alpha^{(c)}$ and $\beta^{(c)}$.

3. Strength Estimation

The strength estimation is based on the J_2 yield criterion, i.e. that only the deviatoric part of the imposed load can cause a failure of the material. Therefore, it is necessary to calculate the deviatoric stress in individual components, which can be afterwards compared with a critical stress. Such approach was used by Pichler and Hellmich (2011) and it turned out to be suitable for an estimation of the compressive strength in cementitious materials.

Due to the assumed elastic linear behavior of the RVE, all imposed work is stored at each point as an elastic energy density, $W_\mathrm{e} = 1/2\,\boldsymbol{\sigma} : \boldsymbol{\varepsilon} = 1/2\,\boldsymbol{\varepsilon} : \mathbf{L} : \boldsymbol{\varepsilon}$, which can be decomposed into the volumetric and deviatoric parts, $W_\mathrm{e} = 1/2\,\sigma_\mathrm{m}\varepsilon_\mathrm{V} + 1/2\,\mathbf{s} : \mathbf{e}$. The quantity $\varepsilon_\mathrm{V} = 1/3\,\boldsymbol{\delta} : \boldsymbol{\varepsilon}$ represents the relative change of volume, $\mathbf{e}$ is obtained as $\mathbf{e} = \boldsymbol{\varepsilon} - \boldsymbol{\delta}\varepsilon_\mathrm{V}$ and it represents the deviatoric part of the strain tensor, $\sigma_\mathrm{V} = 1/3\,\boldsymbol{\delta} : \boldsymbol{\sigma}$ is the mean stress and $\mathbf{s} = \boldsymbol{\sigma} - \boldsymbol{\delta}\sigma_\mathrm{V}$ is the stress deviator.

The deviatoric part of the imposed work, $W_\mathrm{eD} = 1/2\,\mathbf{s} : \mathbf{e} = 1/(4G)\,\mathbf{s} : \mathbf{s}$, is proportional to the second invariant of the stress deviator, J_2, where

$$J_2 = 1/2\,\mathbf{s} : \mathbf{s} \tag{20}$$

and therefore $W_\mathrm{eD} = J_2/(2G)$. The quadratic average of the deviatoric stress is then $\|\mathbf{s}\| = \sqrt{2\,J_2}$

3.1. Quadratic Strain Averages

The expression for the quadratic average of the deviatoric strain field over a general phase, r, can be derived using the Hill's lemma

$$\langle U \rangle = \frac{1}{2}\langle \mathbf{E}^{(r)} : \mathbf{L}^{(r)} : \mathbf{E}^{(r)} \rangle = \frac{1}{2}\langle \mathbf{E}^{(r)} \rangle : \mathbf{L}^{\mathrm{eff}} : \langle \mathbf{E}^{(r)} \rangle = \frac{1}{2}\mathbf{E} : \mathbf{L}^{\mathrm{eff}} : \mathbf{E} \tag{21}$$

which expresses the equality between the average strain energy density, $\langle U \rangle$, in the RVE by means of the microscopic or macroscopic quantities (Gross and Seelig, 2006). From Eq. (21) the following equality can be obtained:

$$\mathbf{E} : \mathbf{L}^{\mathrm{eff}} : \mathbf{E} = \frac{1}{|\Omega|}\int_\Omega \boldsymbol{\varepsilon}(\mathbf{x}) : \mathbf{L}(\mathbf{x}) : \boldsymbol{\varepsilon}(\mathbf{x})\,\mathrm{d}\mathbf{x} \tag{22}$$

where Ω stands for the domain of the entire RVE, opposed to $\Omega^{(r)}$ denoting the domain of the single inclusion (inhomogeneity). The local strain $\boldsymbol{\varepsilon}(\mathbf{x})$ can be then decomposed into its volumetric and deviatoric part (responsible for the material failure):

$$\mathbf{E} : \mathbf{L}^{\mathrm{eff}} : \mathbf{E} = \frac{1}{|\Omega|}\int_\Omega \boldsymbol{\varepsilon}(\mathbf{x}) : [K(\mathbf{x})\mathbf{I}_\mathrm{V} + 2G(\mathbf{x})\mathbf{I}_\mathrm{D}] : \boldsymbol{\varepsilon}(\mathbf{x})\,\mathrm{d}\mathbf{x} \tag{23}$$

To extract the deviatoric part, it is convenient to differentiate the entire expression (23) with respect to $G^{(r)}$. The volumetric part vanishes and we obtain

$$\mathbf{E} : \frac{\partial \mathbf{L}^{\text{eff}}}{\partial G^{(r)}} : \mathbf{E} = \frac{1}{|\Omega|} \sum_{r=0}^{n} \int_{\Omega^{(r)}} 2\, \mathbf{e}^{(r)}(\mathbf{x}) : \mathbf{e}^{(r)}(\mathbf{x})\, \mathrm{d}\mathbf{x} \tag{24}$$

which can be after a simple manipulation:

$$\frac{1}{2}\, \mathbf{E} : \frac{\partial \mathbf{L}^{\text{eff}}}{\partial G^{(r)}} : \mathbf{E} = \frac{1}{|\Omega|} \frac{|\Omega^{(r)}|}{|\Omega^{(r)}|} \sum_{r=0}^{n} \int_{\Omega^{(r)}} \mathbf{e}^{(r)}(\mathbf{x}) : \mathbf{e}^{(r)}(\mathbf{x})\, \mathrm{d}\mathbf{x} \tag{25}$$

knowing that $c^{(r)} = |\Omega^{(r)}|/|\Omega|$, even more simplified:

$$\frac{1}{2}\, \mathbf{E} : \frac{\partial \mathbf{L}^{\text{eff}}}{\partial G^{(r)}} : \mathbf{E} = c^{(r)} \frac{1}{|\Omega^{(r)}|} \int_{\Omega^{(r)}} \mathbf{e}^{(r)}(\mathbf{x}) : \mathbf{e}^{(r)}(\mathbf{x})\, \mathrm{d}\mathbf{x} \tag{26}$$

The quadratic average of the deviatoric strain field over a general phase, r, is defined as (Pichler and Hellmich, 2011)

$$\|\mathbf{e}^{(r)}\| = \sqrt{\frac{1}{|\Omega^{(r)}|} \int_{\Omega^{(r)}} \frac{1}{2}\, \mathbf{e}^{(r)}(\mathbf{x}) : \mathbf{e}^{(r)}(\mathbf{x})\, \mathrm{d}\mathbf{x}} \tag{27}$$

and using Eq. (26), it can be also expressed as

$$\|\mathbf{e}^{(r)}\| = \sqrt{\frac{1}{4c^{(r)}}\, \mathbf{E} : \frac{\partial \mathbf{L}^{\text{eff}}}{\partial G^{(r)}} : \mathbf{E}} \tag{28}$$

The related quadratic average of the deviatoric stress field (see (20)) is used as an estimate for deviatoric stress peaks (Pichler and Hellmich, 2011):

$$\|\mathbf{s}^{(r)}\| = \sqrt{\frac{1}{|\Omega^{(r)}|} \int_{\Omega^{(r)}} \frac{1}{2}\, \mathbf{s}^{(r)}(\mathbf{x}) : \mathbf{s}^{(r)}(\mathbf{x})\, \mathrm{d}\mathbf{x}} = 2G^{(r)} \|\mathbf{e}^{(r)}\| \tag{29}$$

Assuming the elasto-brittle behavior, the elastic response can be expected until the quadratic deviatoric stress averages over each of the phases remain below a critical strength (Pichler and Hellmich, 2011):

$$\|\mathbf{s}^{(r)}\| \leq s_{\text{crit}}^{(r)} \tag{30}$$

4. Homogenization of Cocciopesto Mortar

The specific feature of cocciopesto mortars is that a thin layer of C-S-H gel is formed around the crushed brick particles and it should be taken into account in the calculation. A thickness of the C-S-H layer at the brick interface is assumed to be about 20 μm for the calculations; the backscattered electron image of the interface can be seen in Fig. 2, which is reproduced from Böke et al. (2006). However, the estimation of the C-S-H gel thickness on the brick interface is one of the deficiencies in the modeling. Another uncertainty is the elastic stiffness of the gel. There are basically two types of the gel present in the Portland cement. As reported in literature, e.g. Selvam et al. (2009), these are low and high-density C-S-H gel. For the calculation of the effective properties of cocciopesto mortars, values representing the low-density C-S-H gel were considered. The nanoindentation results showed that the low-density C-S-H phase has a mean stiffness of about 22 GPa (Constantinides and Ulm, 2004), the density of the gel in calculation was considered as 2000 $\mathrm{kg/m^3}$, as suggested in Jeffrey and Hamlin (2006) and Poisson's ratio as 0.20.

In the calculations it is assumed that 50% of the C-S-H gel occupies the voids, 30% of the C-S-H gel consumes a part of the lime matrix and the remaining 20% is assumed to consume a part of the brick phase. These values are only estimated, but they do not have any significant influence on the final results. Despite the uncertain material properties of the gel phase, the model should be capable to indicate trends.

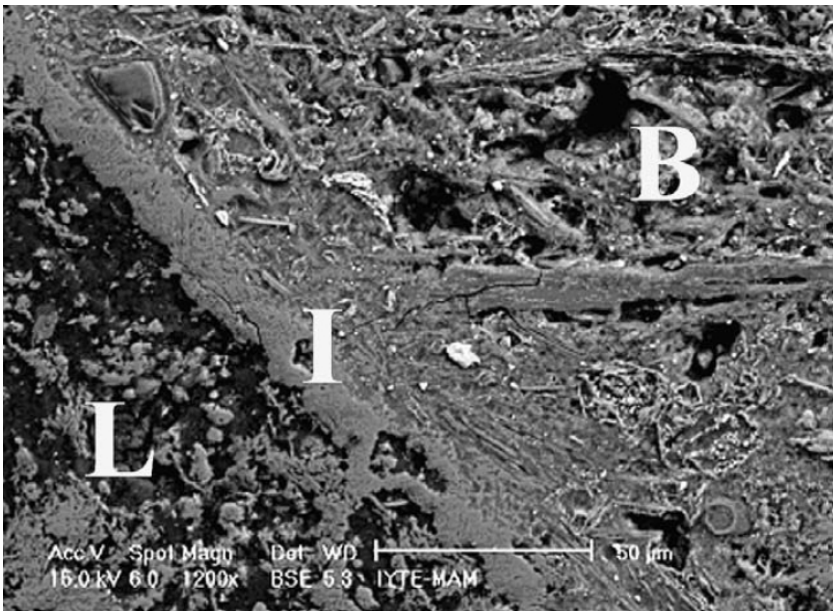

Fig. 2: Brick interface (I) between lime matrix (L) and brick aggregate (B), reproduced from Böke et al. (2006)

Based on a comprehensive literature study, e.g. Maropoulou et al. (2005), the mix proportions for the micromechanical homogenization of the cocciopesto mortar were determined as 4 mass portions of lime matrix, 3 mass portions of crushed bricks and 5 mass portions of siliceous sand in the hardened mortar. This composition should be similar to the historic mortars described by, for instance, Vitruvius. A porosity of the hardened mortar is varying according to the environment and technology. For the calculations, the porosity was considered to be 30% of the volume. The mechanical properties of the individual components, considered in the calculations, are summarized in Tab. 1. The properties of voids are set to be non-zero to avoid numerical complications.

Tab. 1: Properties of individual components used for calculations

	density	E	ν	tensile strength	source
	$[\mathrm{kg/m^3}]$	[MPa]	-	[MPa]	-
lime	1900	1800	0.25	0.4	Drdácký and Michoinová (2003)
siliceous sand	2600	70000	0.17	48	AZoM (2012)
clay brick	1600	2400	0.17	3.2	Hendricx et al. (2009)
voids	-	10^{-9}	10^{-3}	-	-

The summary of material properties in Tab. 1 indicates that the weakest constituent is the hardened lime matrix, having the tensile strength approximately 0.4 MPa. This value can vary according to curing time and technology. However, the value should not be higher than 0.7 MPa, which is still way smaller than the tensile strength of the other components.

4.1. Results and Discussion

The C-S-H gel coating significantly stiffens the crushed brick particles and its presence results in an increase of the effective mortars stiffness (see Fig. 3), even though the layer is relatively thin in comparison with the diameter of the brick particles.

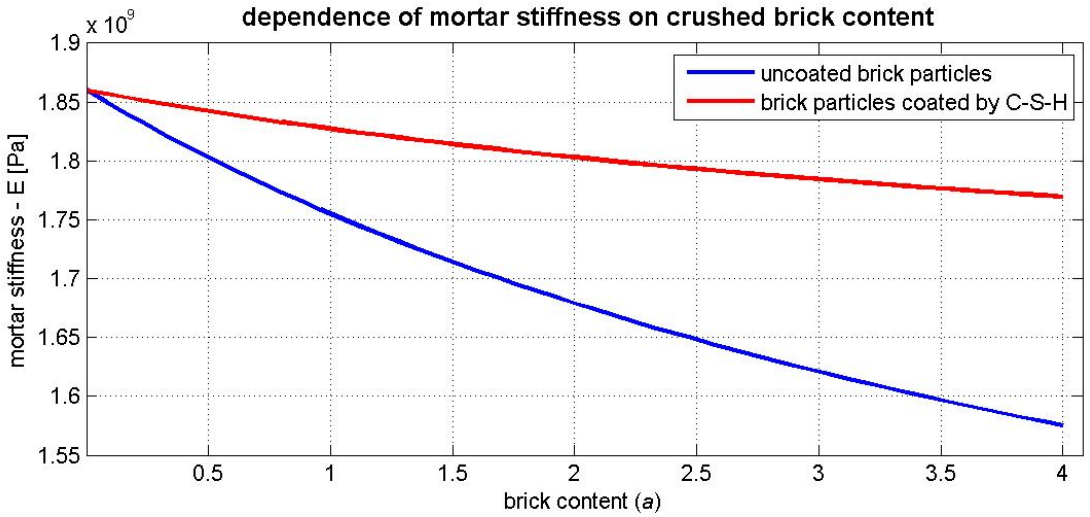

Fig. 3: The effective stiffness of mortars containing coated / uncoated crushed brick particles

It can be clearly seen from Fig. 3 that with the addition of crushed bricks without consideration of coating, the mortar stiffness is quite significantly reduced. However, for the mortar containing coated crushed brick particles the mortar stiffness reduction or increase is strongly dependent on the size of the added crushed brick particles. The variable parameter a (brick content) has a meaning of the mass portion in the mix (lime : brick : sand = 4 : a : 5). The calculation were done assuming the size of the brick particles to be 1 mm in diameter. From the nature of the Mori-Tanaka method, the crushed brick size distribution does not have any effect in case of uncoated particles, but plays a significant role in case of particles with coating.

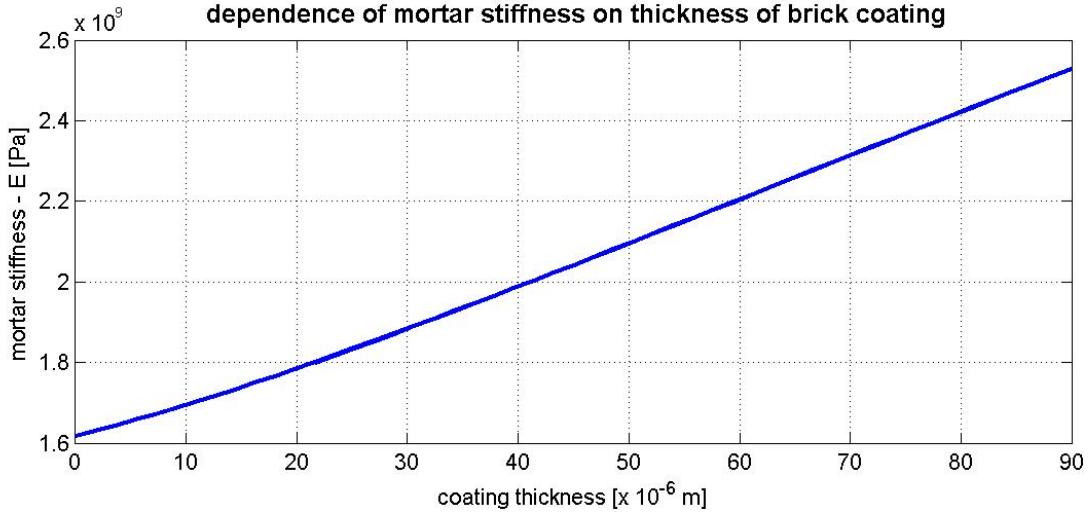

Fig. 4: A dependence of the effective mortar stiffness on coating thickness

If the C-S-H gel coating is formed, a bigger coating thickness should result in an increase of the effective mortar stiffness (see Fig. 4). The same increase of the effective mortar stiffness can be obtained if smaller crushed brick particles are added (see Fig. 5).

It can be concluded that the C-S-H gel formation on the interface of crushed brick particles results in an increase of the effective mortar stiffness. This increase is steep if the ratio of gel thickness to size of brick particles is relatively high (see Fig. 5), and that can be ensured by addition of crushed brick particles having a smaller diameter.

A reduction or increase of the deviatoric stress in the lime matrix is also strongly dependent on the ratio of coating thickness to size of crushed brick particles. If the added brick particles are smaller, the

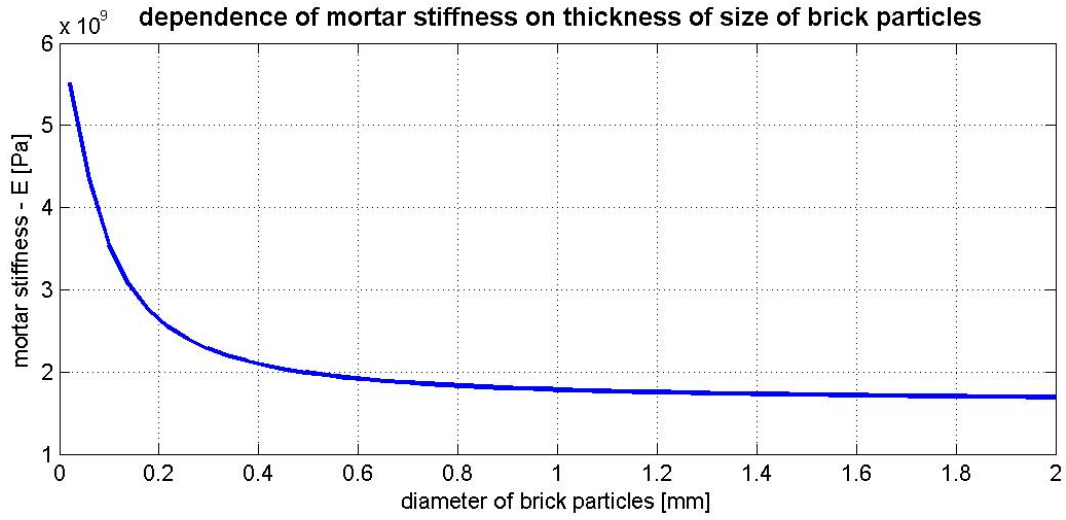

Fig. 5: A dependence of the effective mortar stiffness on a diameter of brick particles

effect of C-S-H gel coating becomes greater and the deviatoric stress within the lime matrix significantly decreases (see Fig. 6). The values on the y-axis in Fig. 6 represent the ratio of the quadratic average of the deviatoric stress in the lime matrix for particles approaching zero diameter (being the reference value), $\|\mathrm{s}^{(0)}(r \to 0)\|$, to the quadratic average of the deviatoric stress in the lime matrix for crushed brick particles of a variable size (on the x-axis), $\|\mathrm{s}^{(0)}\|$.

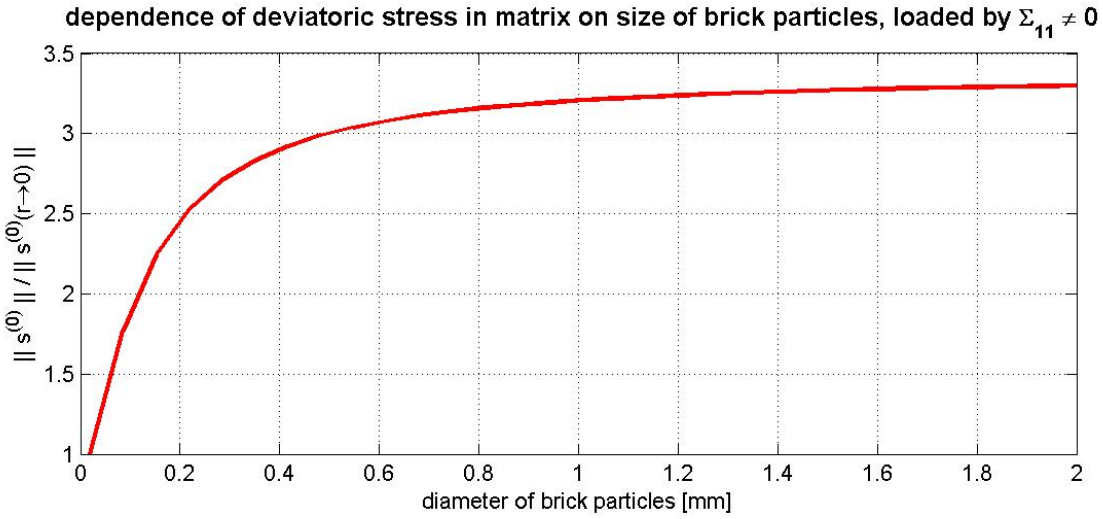

Fig. 6: A dependence of the deviatoric stress in matrix on a diameter of brick particles

From the calculations it seems reasonable to add a certain amount of finely ground bricks into to the mix, since it should result in a reduction of the deviatoric stress within the matrix. It can be concluded that big-size brick particles cause a mortar stiffness decrease and the small particles are responsible for a reduction the deviatoric stress in lime matrix. This reduction can be seen in Fig. 7, where the uniform crushed brick size distribution was modified in order to reduce the deviatoric stress in the lime matrix and to keep the mortar stiffness as low as possible. While in case of the uniform crushed brick size distribution the deviatoric stress within the lime matrix is increasing with the addition of crushed brick particles, it is being reduced with the addition of crushed bricks having a smaller diameter.

For the conservation mortars a low elastic modulus and sufficient strength are, together with ductility, usually required (Velosa et al., 2009). The proper composition of a mortar can be prepared using multiple fractions of crushed bricks. Fine brick particles in the mix should ensure a reduction of the deviatoric

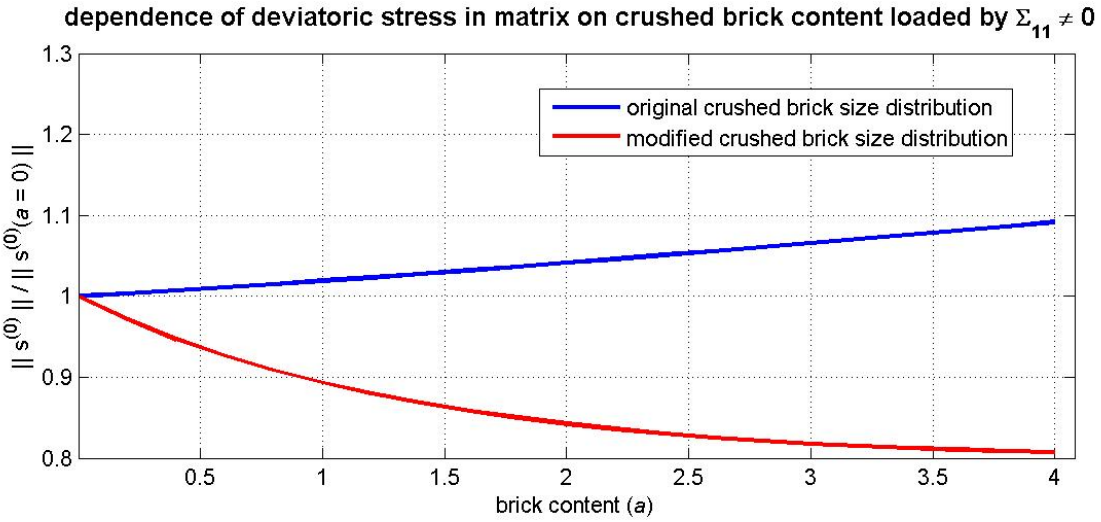

Fig. 7: A comparison of a uniform and modified size distribution crushed brick particles

stress in matrix, and therefore increase the mortar strength. On the other hand, bigger fractions make the mortar more compliant.

5. Conclusions

The calculations based on micromechanical approach revealed, confirmed or provided an explanation to the following facts:

- The assumption of C-S-H gel formation on the matrix-crushed brick interface has a major influence on behavior of the cocciopesto mortars, especially in case of small crushed brick fractions.
- The main factor influencing the behavior of the crushed bricks (or other clay products, such as tiles or pottery) in a mortar is the ratio of coating thickness to crushed brick size. It was also found that the addition of crushed bricks, having a bigger diameter, should make the mortar more compliant and cause an increase of the deviatoric stress in the matrix. The addition of crushed bricks of a small size results in the opposite behavior - the mortar becomes stiffer and the deviatoric stress in the lime matrix is reduced, ensuring a higher mortar strength.
- The proposed model also confirmed a negative effect of voids in lime mortars, since the increased porosity causes quite large increase of the deviatoric stress within the lime matrix, and therefore reduces the mortar strength (Nežerka, 2011).

However, the results provided in this work, cannot be considered as exact because of a few simplifications and uncertainties in the calculation. The Mori-Tanaka homogenization technique assumes the materials to behave linearly and it is expected that the C-S-H gel should have additional positive effect on the mortar strength if the non-linear behavior were considered. The thickness of the C-S-H gel coating, 20 μm, cannot be also taken as the exact universal value, since it is dependent on the amount and a chemical composition of the individual mortar constituents. There is also uncertainty around the reduction of porosity, if the C-S-H gel is formed.

Acknowledgments

The authors would like to thank for the financial support by the grant no. DF11P01OVV008.

References

AZoM, m. (2012). *Material Science publishing and information provision*. http://www.azom.com/article.aspx?ArticleID=1114.

Baronio, G., Binda, L., and Lombardini, N. (1997). The role of brick pebbles and dust in conglomerates based on hydrated lime and crushed bricks. *Construction and Building Materials*, 11:33–40.

Benveniste, Y. (1987). A new approach to the application of Mori-Tanaka theory in composite materials. *Mechanics of Materials*, 6:147–157.

Böke, H., Akkurt, S., Ípekoğlu, B., and Uğurlu, E. (2006). Characteristics of brick used as aggregate in historic brick-lime mortars and plasters. *Cement and Concrete Research*, 36:1115–1122.

Constantinides, G. and Ulm, F. (2004). The effect of two types of C-S-H on the elasticity of cement-based materials: Results from nanoindentation and micromechanical modeling. *Cement and Concrete Research*, 34:67–80.

Drdácký, M. and Michoinová, D. (2003). Lime mortars with natural fibres. *Britle Matrix Composites 7" Proceedings of the 7th Int. Symposium*, pages 523–532.

Gross, D. and Seelig, T. (2006). *Fracture Mechanics with an Introduction to Micromechanics*. Springer.

Hendricx, R. et al. (2009). Observation of the failure mechanism of brick masonry doublets with cement and lime mortars by X-ray CT. Technical report, Katholieke Universiteit Leuven.

Jeffrey, J. and Hamlin, M. (2006). A colloidal interpretation of chemical aging of the c-s-h gel and its effects on the properties of cement paste. *Cement and Concrete Research*, 36:30–38.

Luo, H. and Weng, G. (1987). On Eshelby's inclusion problem in a three-phase spherically concentric solid, and a modification of Mori-Tanaka's method. *Mechanics of Materials*, 6:347–361.

Maropoulou, A., Bakolas, A., and Anagnostopoulou, S. (2005). Composite materials in composite structures. *Cement and Concrete Composites*, 27:295–300.

Maropoulou, A., Bakolas, A., and Bisbikou, K. (1995). Characterization of ancient, Byzantine and later historic mortars by thermal and X-ray diffraction techniques. *Thermochemica Acta*, 269/270:779–995.

Mori, T. and K., T. (1973). Average stress in matrix and average elastic energy of materials with mixfitting inclusions. *Acta Metallurgica*, 21:571–574.

Mura, T. (1987). *Micromechanics of Defects in Solids*. Springer.

Nežerka, V. (2011). Micromechanics-Based Models of Cocciopesto Mortars. Master's thesis, Czech Technical University in Prague.

Pichler, B. and Hellmich, C. (2011). Upscaling quasi-brittle strength of cement paste and mortar: A multi-scale engineering mechanics model. *Cement and Concrete Research*, 41:467–476.

Selvam, P., Subramani, V., Murray, S., and Hall, K. (2009). *Potential Application of Nanotechnology on Cement Based Materials*. Mack-Blackwell Rural Transportation Center.

Velosa, A., Rocha, F., and Veiga, R. (2009). Influence of chemical and mineralogical composition of metakaolin on mortar characteristics. *Acta Geodynamica et Geomaterialia*, 153:121–126.

Šmilauer, V., Hlaváček, P., Škvára, F., Šulc, R., Kopecký, L., and Němeček, J. (2011). Micromechanical multiscale model for alkali activation of fly ash and metakaolin. *Journal of Materials Science*, pages 1–11.

Appendix

The individual matrices, needed for the calculation of coefficients a_1, a_2 and b_1, b_2 that are necessary for the determination of the deviatoric constraint constants (see Section 2.3.), can be found as

$$\mathbf{E} = \begin{bmatrix} 1 & -\dfrac{6\nu^{(c)}}{1-2\nu^{(c)}} & 3 & \dfrac{5-4\nu^{(c)}}{1-2\nu^{(c)}} \\ 1 & -\dfrac{7-4\nu^{(c)}}{1-2\nu^{(c)}} & -2 & 2 \\ 1 & \dfrac{3\nu^{(c)}}{1-2\nu^{(c)}} & -12 & \dfrac{-2\left(5-\nu^{(c)}\right)}{1-2\nu^{(c)}} \\ 1 & -\dfrac{7+2\nu^{(c)}}{1-2\nu^{(c)}} & 8 & \dfrac{2\left(1+\nu^{(c)}\right)}{1-2\nu^{(c)}} \end{bmatrix} \tag{31}$$

$$\mathbf{F} = \begin{bmatrix} 3 & \dfrac{5-4\nu^{(m)}}{1-2\nu^{(m)}} \\ -2 & 2 \\ -\dfrac{12G^{(m)}}{G^{(c)}} & \dfrac{-2\left(5-\nu^{(m)}\right)}{1-2\nu^{(m)}}\dfrac{G^{(m)}}{G^{(c)}} \\ \dfrac{8G^{(m)}}{G^{(c)}} & \dfrac{2\left(1+\nu^{(m)}\right)}{1-2\nu^{(m)}}\dfrac{G^{(m)}}{G^{(c)}} \end{bmatrix} \tag{32}$$

$$\mathbf{H} = \begin{bmatrix} 1 & -\dfrac{6\nu^{(g)}}{1-2\nu^{(g)}} \\ 1 & -\dfrac{7-4\nu^{(g)}}{1-2\nu^{(g)}} \end{bmatrix} \tag{33}$$

$$\mathbf{K} = \mathbf{G}\mathbf{E}^{-1}\mathbf{F} \tag{34}$$

$$\mathbf{R} = \mathbf{P} + \mathbf{Q}\mathbf{E}^{-1}\mathbf{F}\mathbf{K}^{-1}\mathbf{H} \tag{35}$$

where

$$\mathbf{G} = \begin{bmatrix} 1 & -\dfrac{6\nu^{(c)}c^{\,2/3}}{1-2\nu^{(c)}} & \dfrac{3}{c^{\,5/3}} & \dfrac{5-4\nu^{(c)}}{\left(1-2\nu^{(c)}\right)c} \\ 1 & -\dfrac{\left(7-4\nu^{(c)}\right)c^{\,2/3}}{1-2\nu^{(c)}} & -\dfrac{2}{c^{\,5/3}} & \dfrac{2}{c} \end{bmatrix} \tag{36}$$

$$\mathbf{P} = \begin{bmatrix} 1 & \dfrac{3\nu^{(g)}}{1-2\nu^{(g)}} \\ 1 & -\dfrac{7+2\nu^{(g)}}{1-2\nu^{(g)}} \end{bmatrix} \tag{37}$$

and finally

$$\mathbf{Q} = \frac{G^{(c)}}{G^{(g)}} \begin{bmatrix} -1 & -\dfrac{3\nu^{(c)}c^{\,2/3}}{1-2\nu^{(c)}} & \dfrac{12}{c^{\,5/3}} & \dfrac{2\left(5-\nu^{(c)}\right)}{\left(1-2\nu^{(c)}\right)c} \\ -1 & \dfrac{\left(7+2\nu^{(c)}\right)c^{\,2/3}}{1-2\nu^{(c)}} & -\dfrac{8}{c^{\,5/3}} & \dfrac{2\left(1+\nu^{(c)}\right)}{\left(1-2\nu^{(c)}\right)c} \end{bmatrix} \tag{38}$$